J. Physiol. (1961), **156**, *pp.* 389–414
With 16 *text-figures*
Printed in Great Britain

EFFECT OF BARIUM IONS ON MEMBRANE POTENTIALS OF COCKROACH GIANT AXONS

BY T. NARAHASHI*

From the Laboratory of Applied Entomology, Faculty of Agriculture, University of Tokyo, Japan

(*Received* 19 *December* 1960)

There is evidence that barium ions may be substituted for sodium ions to produce action potentials in crustacean muscle fibres (Fatt & Ginsborg, 1958) and in mammalian B and C fibres (Greengard & Straub, 1959). In these fibres the action potentials are remarkably prolonged in an isotonic barium solution. In mammalian A fibres, however, barium cannot be substituted for sodium, and isotonic barium causes conduction block (Greengard & Straub, 1959).

A series of investigations on the excitation and electrical properties of cockroach giant axons has revealed that they resemble in many respects the giant axons of the squid, which have been widely regarded as representative of non-myelinated nerve fibres (Narahashi, 1960*a*). For example, the membrane potential of cockroach giant axons behaves quite similarly to that of squid giant axons with various external concentrations of sodium and potassium (Yamasaki & Narahashi, 1958, 1959*a*), and the negative after-potential can be explained on the same basis (Narahashi & Yamasaki, 1960*a*). It is therefore interesting to examine the behaviour of the membrane potential of this non-myelinated nerve fibre under the influence of barium.

Attention has recently been focused on the nature of the after-potential as well as on that of the spike potential. There have appeared many publications dealing with the augmentation and prolongation of the negative after-potential under a variety of experimental conditions (see Shanes, 1958). In the giant axons of the cockroach the negative after-potential is increased by treatment with calcium-rich solutions and the insecticides dicophanum (DDT) and allethrin (synthetic pyrethrin) (Narahashi, 1960*a*, *b*; Narahashi & Yamasaki, 1960*b*, *c*). Barium also increases the negative after-potential of the giant axon of the cockroach and an attempt was made to elucidate the mechanism of this increase.

* Address for 1961: Department of Physiology, University of Chicago, Chicago 37, Illinois, U.S.A.

METHODS

The giant axons in the abdominal nerve cord of the American cockroach, *Periplaneta americana* L., were used throughout the experiments. The methods of stimulation and recording were essentially similar to those described in the previous paper (Narahashi & Yamasaki, 1960*a*). External stimulation was effected by a pair of silver-wire electrodes, while recordings were made by a micro-electrode inserted in the desheathed region of an axon. In the present experiments, however, an additional micro-electrode was often inserted in the same axon within 50 μ of the recording electrode in order to deliver polarizing current. The voltage drop across a resistor connected in series with the current-passing electrode gave a measure of current strength. Micro-electrodes having a resistance of 10–20 MΩ were selected for both polarization and recording. The input stray capacity was compensated by a negative-capacity feedback amplifier, the rising phase of a recorded square pulse of current being reduced to less than 10 μsec when the above-mentioned micro-electrodes were used.

TABLE 1. Composition of solutions (mM)

	Na	Ba	Sucrose	K	Ca	Cl	HCO_3
Normal	214	0	0	3·1	1·8	220·7	0·5
150 mM-Na	150	0	128	3·1	1·8	156·7	0·5
150 mM-Na + 21 mM-Ba	150	21	64	3·1	1·8	198·7	0·5
150 mM-Na + 43 mM-Ba	150	43	0	3·1	1·8	242·7	0·5
100 mM-Na	100	0	227	3·1	1·8	106·7	0·5
100 mM-Na + 21 mM-Ba	100	21	163	3·1	1·8	148·7	0·5
100 mM-Na + 43 mM-Ba	100	43	98	3·1	1·8	192·7	0·5
100 mM-Na + 76 mM-Ba	100	76	0	3·1	1·8	258·7	0·5
75 mM-Na	75	0	278	3·1	1·8	81·7	0·5
75 mM-Na + 93 mM-Ba	75	93	0	3·1	1·8	267·7	0·5
50 mM-Na	50	0	328	3·1	1·8	56·7	0·5
50 mM-Na + 109 mM-Ba	50	109	0	3·1	1·8	274·7	0·5
Isotonic Ba	0	143	0	3·1	1·8	292·7	0·5

pH: *ca.* 7·2.

The Ringer's solution was the same as that described in the previous paper (Narahashi & Yamasaki, 1960*a*) except that phosphates were replaced by bicarbonate as a buffer. When the effect of barium was to be examined, sodium was replaced by barium, keeping the solution isotonic. A sucrose Ringer's solution in which the corresponding amount of sodium was replaced by sucrose was used as a control in addition to normal Ringer's solution. The concentrations of potassium and calcium were kept constant in all modified Ringer's solutions, including isotonic Na-free Ba-Ringer's solution. The composition of the solutions used is given in Table 1.

Since the micro-electrodes were kept inserted while the bathing fluid was changed by continuous perfusion, as described previously (Narahashi & Yamasaki, 1960*a*), the resting potential in the test solutions was measured in the following way. The input circuit, when an axon is impaled by the recording micro-electrode consists of the following: grid of cathode follower—Ag-AgCl—3 M-KCl (micro-electrode)—axoplasm—nerve membrane—bathing fluid—agar-Ringer—3 M-KCl—Ag-AgCl—ground. While the recording micro-electrode was kept inserted in an axon, the input of the recording system was grounded at intervals and the resulting difference in potential, 'apparent resting potential', was measured. This value was the sum of the resting potential, the tip potential of micro-electrode, and the potentials produced at the other interphases of the input circuit. The latter potentials included those produced at the junctions between the Ag-AgCl and the

3 M-KCl in the micro-electrode, between the bathing fluid and the agar-Ringer of the indifferent electrode, between the agar-Ringer and the 3 M-KCl in the indifferent electrode, and between the 3 M-KCl and the Ag-AgCl of the indifferent electrode. At the end of each experiment the recording micro-electrode was withdrawn in normal Ringer's solution and the potential change was measured. This value gave the resting potential measured directly at that moment. Furthermore, the input was grounded while the tip of the micro-electrode just withdrawn from the axon was in normal Ringer's solution, and the potential change was measured. This value gave the sum of the tip potential and the other junction potentials, and was therefore subtracted from all measurements of the apparent resting potential made during the course of the experiment. Since the resistance of the micro-electrode was relatively low, it could be assumed that the magnitude of the tip potential measured in axoplasm was the same as it was in bathing fluid, and that the tip potential was constant throughout the experiment. The measurements in test solutions needed an additional correction. The junction potential between the bathing solution and the agar-Ringer of the indifferent electrode should have changed when the ionic composition of bathing solution was altered. The difference in junction potential was measured in another set of experiments with the test solutions given in Table 1. The recording micro-electrode was replaced by a glass tube of about 8 mm inside diameter in which agar-3-M-KCl and 3 M-KCl solutions were introduced. The input was grounded while the KCl tube was dipped in the bathing fluid, and the potential change was measured. Such a potential obtained in normal Ringer's solution was then subtracted from the potentials in the test solutions. Although the differences were only a few millivolts, they were further subtracted from the apparent resting potentials to obtain the true resting potentials. Despite these corrections, the measurements of the resting potential were less reliable than those of the action potential.

The experiments were conducted during the summer months at room temperatures ranging from 28 to 34·5° C. Although the temperatures were somewhat high, they did not have any harmful effect either on the intact cockroaches or on the isolated nerve cord preparations, the resting and action potentials remaining nearly constant in normal Ringer's solution for over 5 hr.

RESULTS

Resting and action potentials

Isotonic Ba solution. When normal Ringer's solution was replaced with isotonic barium solution, nerve conduction was immediately blocked, but the effect was completely reversible upon washing with normal Ringer's solution.

Solution with 75 mM-Na and 93 mM-Ba. Nerve conduction was also blocked when the concentration of barium was reduced to 93 mM, as is illustrated in Fig. 1. The normal Ringer's solution containing 214 mM-Na was first replaced by 75 mM-Na containing no Ba (records *A* and *B*). The magnitude of the action potential was markedly reduced, and the rate of rise and the rate of fall of the action potential, especially the former, were also decreased, but the positive phase which followed the spike phase remained almost unchanged. This observation is in good agreement with that made previously (Yamasaki & Narahashi, 1958, 1959*a*). When the bathing fluid was then changed to 75 mM-Na + 93 mM-Ba, the action potential became double-peaked and finally conduction was blocked, leaving only a small residual potential (record *C*). The graded nature of

the change was undoubtedly due to slow exchange of the bathing fluid. The double-peaked action potential is likely to be a manifestation of saltatory conduction across the desheathed region of the nerve cord where the micro-electrode is inserted, because the nerve sheath provides a strong

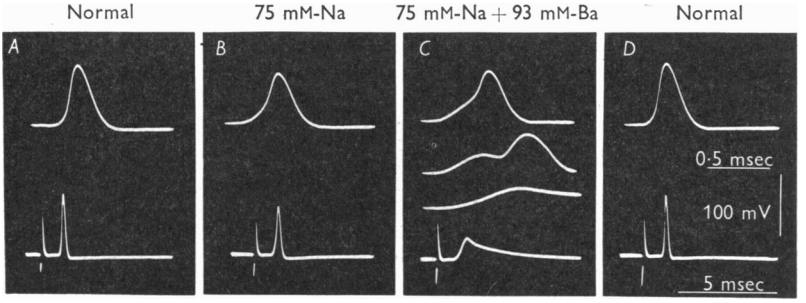

Fig. 1. Records of the action potential showing the effect of reducing Na and adding Ba. In column *C* three records were taken with fast sweep during the course of and after conduction block, and the bottom record was taken with slow sweep after conduction block. Axon 10*d*. Temperature 31·5° C.

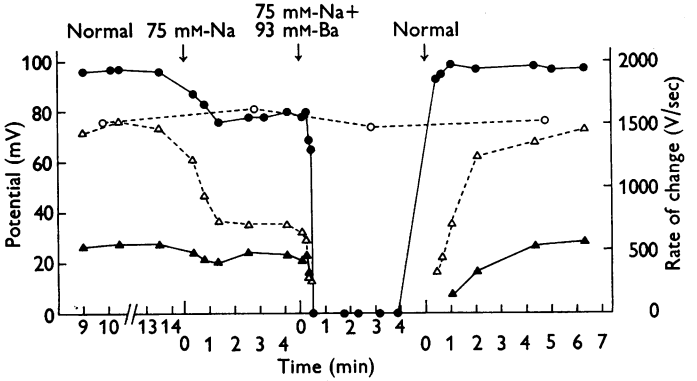

Fig. 2. Changes in the resting potential (○), and in the amplitude (●), the maximum rates of rise (△) and of fall (▲) of the action potential by a reduction of Na and an addition of Ba. Axon 10*d*. Temperature 31·5° C.

barrier against the penetration of ions (Yamasaki & Narahashi, 1959*a*). The effect was completely reversible on washing with normal Ringer's solution (record *D*). An example of the full course of an experiment is presented in Fig. 2, in which the magnitudes of the resting and action potentials and the maximum rates of rise and fall of the action potential are plotted against time. The resting potential was slightly increased by

75 mM-Na and slightly decreased by 75 mM-Na + 93 mM-Ba, but the decrease was too small to account for the conduction block.

Solutions with 100 mM-Na and various concentrations of Ba. The effects of various concentrations of barium contained in 100 mM-Na Ringer's solution are shown in Figs. 3 and 4. Replacement of normal Ringer's solution with 100 mM-Na caused the spike amplitude to decrease. When 21 mM-Ba was added to 100 mM-Na, the resting potential was somewhat

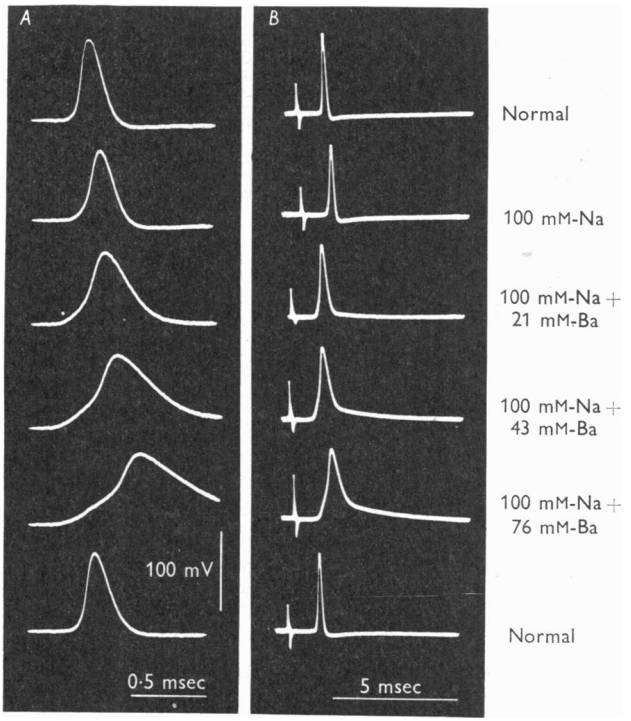

Fig. 3. Records of the action potential in various concentrations of Ba. Both fast (*A*) and slow (*B*) sweep records are shown in each solution. Axon 13*b*. Temperature 34·5° C.

reduced, whereas the height of the action potential increased slightly. Both rising and falling phases of the action potential were slowed down considerably. Another conspicuous change was the reversal of the slow phase following the spike potential, the positive phase being converted into a negative after-potential. Increase in barium concentration to 43 mM and then to 76 mM brought about further accentuation of these effects, except for the effect on the spike amplitude which was nearly unchanged. At these concentrations of barium there appeared a remarkable step on the rising phase of the action potential (Fig. 3). This can be accounted for by

supposing that an action potential originating in the intact region of the nerve cord, where barium has not yet come into contact with the axon because of the barrier of the nerve sheath, spreads electrotonically along the axon to the point of impalement where the nerve has been desheathed and thereby is under the influence of barium, and that the critical depolarization for firing is greatly augmented by barium, as will be described in a later section. All these effects of barium were completely reversed when normal Ringer's solution was introduced into the bathing chamber. The mean values for the amplitude and the maximum rates of rise and fall of the action potential are given in Table 2.

It is interesting to note that the amplitude of the action potential increased temporarily above normal upon readmission of normal Ringer's solution (Fig. 4) Such a tendency was observed very often. The most likely explanation is as follows. When the perfusion of normal Ringer's

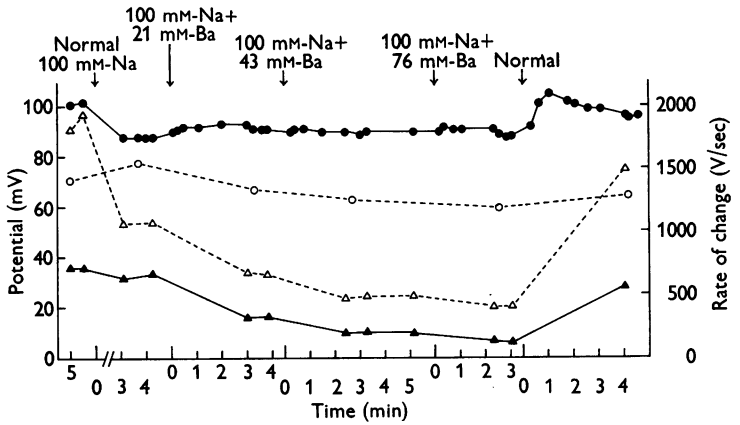

Fig. 4. Changes in the resting potential (○), and in the amplitude (●), the maximum rates of rise (△) and fall (▲) of the action potential in various concentrations of Ba. Axon 13*b*. Temperature 34·5° C.

TABLE 2. Mean values for the amplitude, and the maximum rates of rise and fall of the action potential in various concentrations of Na and Ba. The numbers of measurements are shown in parentheses

	Na concentration (mM)	Ba concentration (mM)			
		0	21	43	76
Amplitude (mV)	214	104 (31)	—	—	—
	150	94 (18)	110 (1)	97 (21)	—
	100	91 (11)	93 (4)	92 (4)	90 (11)
Maximum rate of rise (V/sec)	214	1790 (72)	—	—	—
	150	1350 (8)	800 (1)	790 (7)	—
	100	980 (11)	610 (4)	470 (4)	370 (10)
Maximum rate of fall (V/sec)	214	660 (27)	—	—	—
	150	590 (8)	430 (1)	320 (7)	—
	100	610 (11)	360 (4)	250 (4)	210 (10)

solution is begun, the sodium concentration is progressively raised while the barium concentration is progressively lowered. If the rate at which the action potential was affected by the change in sodium concentration were higher than that at which it was affected by the change in barium concentration, then the rising phase, which is known to be more affected by [Na] than the falling phase (Yamasaki & Narahashi, 1959*a*), would approach the normal level earlier, whereas the falling phase would remain slow both in velocity and in its onset. This would result in an extension of the rising phase beyond its normal level, thereby causing the spike amplitude to increase. After a while, however, the effect of barium on the falling phase would disappear, so that the action potential would revert to its normal shape and magnitude.

Repetitive excitation was rarely induced by a single shock in the barium-treated axons.

Solutions with 150 *mM-Na and various concentrations of Ba.* Experiments similar to those described in the preceding section were carried out using 21 mM- and 43 mM-Ba each contained in 150 mM-Ba. The effect of the barium was essentially the same as before the rising and falling phases of the action potential being slowed down, and the negative after-potential being considerably increased. The increase in spike amplitude by barium was also observed and was more marked than it was in 100 mM-Na. The mean values for the amplitude and the maximum rates of rise and fall of the action potential are given in Table 2.

Critical depolarization and threshold current

Pulses of depolarizing currents of 3 msec duration were delivered through a micro-electrode, and the resulting potentials and the current strengths were recorded. An example of records taken in 150 mM-Na is illustrated in Fig. 5*A*. When the current strength approached threshold, graded responses appeared which terminated in a slight undershoot. At threshold an action potential arose from the top of the graded response and terminated in a marked undershoot. The inflexion point between the slowly rising catelectrotonic potential and the action potential was measured from the resting level and was taken as a measure of the critical depolarization for firing. There was a general tendency for the spike amplitude to become smaller and for the critical depolarization to become slightly higher as the current intensity was reduced. These phenomena are explicable in terms of the inactivation caused by longer lasting cathodal current flow (Hodgkin & Huxley, 1952*a*).

In 150 mM-Na + 43 mM-Ba the critical depolarization was greater, and no undershoot followed the spike, as is shown in Fig. 5*B*.

The mean values for the threshold current and the critical depolariza-

tion are given in Table 3. The critical depolarization increased from 25 to 31 mV on reducing the sodium concentration from 214 mM (normal Ringer) to 150 mM, and concomitantly the threshold current increased from $3{\cdot}4 \times 10^{-8}$ A to $6{\cdot}3 \times 10^{-8}$ A. Barium caused a further increase in critical depolarization to 40 mV, but it had hardly any effect on the threshold current.

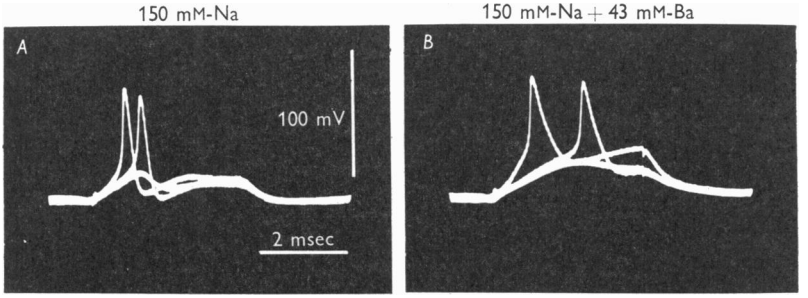

Fig. 5. Records of the catelectrotonic potential and action potential in 150 mM-Na and in 150 mM-Na + 43 mM-Ba. Axon 26. Temperature 32·5° C.

TABLE 3. Critical depolarization and threshold current. Each value represents the mean obtained for one axon by several repeated measurements, the number of which is shown in parentheses. In some axons, several sets of measurements were made at intervals, and the mean values for each set are presented separately

		Normal Ringer's solution		150 mM-Na		150 mM-Na + 43 mM-Ba	
Axon no.	Temp. (°C)	Critical depol. (mV)	Threshold current ($\times 10^{-8}$ A)	Critical depol. (mV)	Threshold current ($\times 10^{-8}$ A)	Critical depol. (mV)	Threshold current ($\times 10^{-8}$ A)
20*a*	29·5	24 (13)	—	—	—	—	—
20*b*	29·5	—	—	—	—	39 (10)	—
		—	—	—	—	36 (5)	—
21	28	24 (5)	3·4 (5)	—	—	—	—
22	28	24 (7)	3·4 (3)	—	—	43 (7)	4·4 (7)
		28 (5)	—	—	—	—	—
23	31	—	—	32 (8)	8·6 (8)	43 (10)	9·3 (5)
24	31	—	—	32 (6)	6·3 (4)	—	—
25	32·5	—	—	33 (7)	6·8 (5)	—	—
26	32·5	—	—	26 (5)	5·0 (5)	42 (4)	4·6 (4)
		—	—	32 (8)	5·0 (8)	41 (4)	5·2 (4)
28	30	—	—	28 (4)	—	35 (4)	—
Mean	30·2	25	3·4	31	6·3	40	5·9

Action potential as affected by the displacement of membrane potential

The total current passing through the nerve membrane can be divided into a capacity current and an ionic current. Thus we have

$$I = C\frac{\mathrm{d}V}{\mathrm{d}t} + I_i,$$

where I is the total membrane current density, I_i is the ionic current density, C is the membrane capacity per unit area, V is the displacement of the membrane potential from its resting value and t is time (Hodgkin & Huxley, 1952*b*). In the case where an action potential is propagated along an axon of uniform structure bathed in a large volume of conducting fluid, the membrane current density is expressed as

$$I = \frac{a}{2R_i\theta^2}\frac{\mathrm{d}^2V}{\mathrm{d}t^2},$$

where a is the radius of the axon, R_i is the specific resistance of the axoplasm and θ is the velocity of conduction (Hodgkin & Huxley, 1952*b*). Hence,

$$I_i = \frac{a}{2R_i\theta^2}\frac{\mathrm{d}^2V}{\mathrm{d}t^2} - C\frac{\mathrm{d}V}{\mathrm{d}t}.$$

Therefore, when the rate of rise of the action potential is at a maximum,

$$I_i = -C\frac{\mathrm{d}V}{\mathrm{d}t}.$$

This means that the ionic current density is proportional to the maximum rate of change of the action potential. In the giant axon of the squid, the inward current upon depolarization is known to be related to the membrane potential immediately before depolarization (Hodgkin & Huxley, 1952*a*). It follows that the rate of rise of the action potential, which is indicative of the inward sodium current, should also be related to the membrane potential from which the action potential arises. This is actually the case in Purkinje fibres (Weidman, 1955).

Now it has been shown that barium causes a slight but definite depolarization. Simultaneously, the rising and falling phases of the spike potential were slowed down. It is therefore reasonable to suppose that the slow rising phase in barium might be due to the fall of resting potential and if this were the case, the rate of rise would be restored by hyperpolarizing the membrane.

Figure 6 illustrates a series of records of the action potential in depolarized (records *A* and *C*) and in hyperpolarized (records *B* and *D*) membranes. In Fig. 7, the height, the maximum rate of rise and the maximum rate of fall of the action potential obtained in normal Ringer's solution and in 150 mM-Na + 43 mM-Ba solution are plotted against the displacement of the membrane potential.

In normal Ringer's solution, the peak of the action potential fell short of the normal level as depolarization became greater (Fig. 6*A*, *b–d*), whereas it could reach almost the normal level even when the membrane was hyperpolarized to a considerable extent (Fig. 6*B*, *a–c*). However,

when the membrane was hyperpolarized still further, the peak of the action potential fell short of the normal level (*Bd*). These effects are more clearly seen in Fig. 7, in which the spike heights measured in normal Ringer's solution (filled-in circles) fall close to a straight line having a slope of about unity in the hyperpolarized membrane, whereas the line bends slightly upwards in the depolarized membrane. The rate of rise of the action potential was lowered very effectively by depolarization (Fig. 6*A* and Fig. 7, filled triangles) this being in good agreement with previous

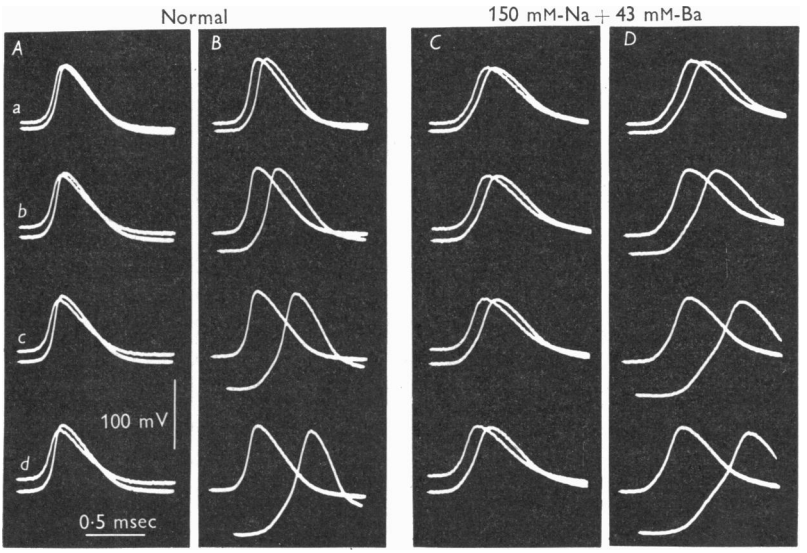

Fig. 6. Effects of depolarization (*A* and *C*) and hyperpolarization (*B* and *D*) on the action potential in normal Ringer's solution and in 150 mM-Na + 43 mM-Ba. The action potential was produced by external stimulation about 20 msec after the onset of polarizing current. In *A* and *C*, the upper trace in each record represents the response in depolarized membrane, and in *B* and *D*, the lower trace is the response in hyperpolarized membrane. Axon 19. Temperature 29·5° C.

observations (Yamasaki & Narahashi, 1959*b*). The rate of rise was also somewhat slowed down by hyperpolarization, although such a slowing was not observed previously (Yamasaki & Narahashi, 1959*b*). The explanation for the discrepancy is not immediately obvious though higher temperature in the present experiments is likely to be one of the factors involved.

On treatment with 150 mM-Na + 43 mM-Ba, there appeared two changes worthy of note. In the first place, the depressive effect of depolarization on the spike height disappeared. The peak of the action potential could now reach its normal level even when the maximum depolarizing current was applied (Fig. 6*C*), so that the curve relating the spike height to the

displacement of the membrane potential became a straight line both in depolarized and in hyperpolarized membranes (Fig. 7, open circles). In the second place, the rate of rise of the action potential became more stable than normal in the sense that the relation with the membrane potential became a straight line with a steep slope, the rising phase now being slightly accelerated by depolarization (Fig. 7, open triangles).

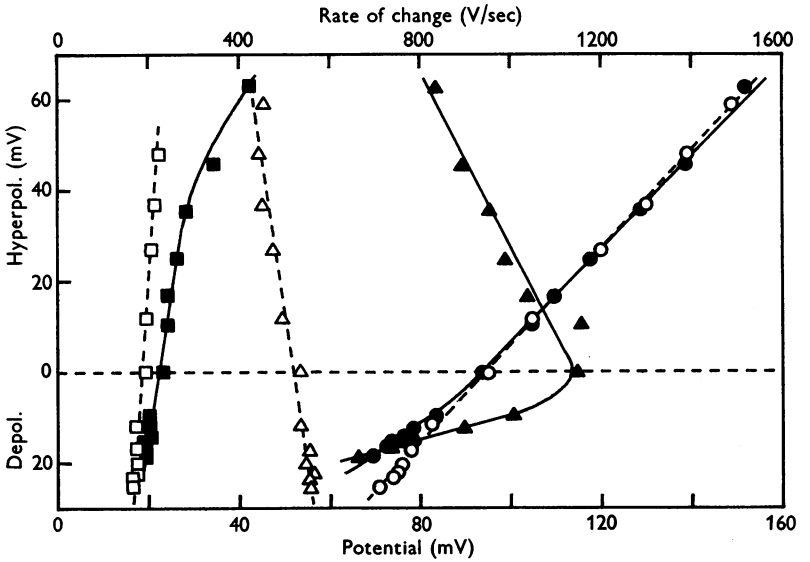

Fig. 7. Changes in the amplitude (○●), and in the maximum rates of rise (△▲) and fall (□■) of the action potential caused by the displacement of the membrane potential from the resting level. The filled symbols represent the measurements in normal Ringer's solution, and the open ones in 150 mM-Na+43 mM-Ba. Axon 19. Temperature 29·5° C.

Although the slowness of the rise of the action potential seems to indicate a reduction of the sodium-carrying system rapidly available upon depolarization, these two features are both well explained by supposing that the inactivation of the sodium-carrying system normally occurring upon depolarization does not take place so effectively as in the normal axons. These observations rule out the possibility that the slowing of the rising phase of the action potential caused by barium is due to the fall of resting potential. There was no marked difference in the rate of fall of the action potential between the normal and Ba-treated axons, except that the absolute value was smaller in the latter (Fig. 7, open squares) than in the former (filled-in squares).

Nature of the negative after-potential increased by Ba

There is good evidence that the negative after-potential of the cockroach giant axon bathed in normal Ringer's solution can be explained by the accumulation of released potassium in the immediate vicinity of the nerve membrane (Narahashi & Yamasaki, 1960*a*). The insecticide DDT has been shown to cause the negative after-potential to increase markedly, and a plateau phase even appeared in the later stages of DDT poisoning if the external potassium was reduced to zero (Narahashi & Yamasaki, 1960*b*, *c*). This increase is explicable on the assumption that the increase in membrane potassium conductance taking place during the latter half of the action potential is delayed and partly suppressed (Narahashi & Yamasaki, 1960*b*), and that in later stages of DDT poisoning a partial suppression of sodium inactivation during the falling phase of the action potential may also be involved (Narahashi & Yamasaki, 1960*c*). An attempt was therefore made to elucidate the mechanism underlying the increase in negative after-potential by barium through the same approach as in the case of DDT.

Addition of negative after-potentials by repetitive stimulation. It is reasonable to assume that the negative after-potentials would add during repetitive excitation if they were due to the accumulation of some substance inside or outside of the membrane. This proved to be the case in squid giant axons (Frankenhaeuser & Hodgkin, 1956), in cockroach giant axons (Narahashi & Yamasaki, 1960*a*) and in mammalian non-myelinated nerve fibres (Greengard & Straub, 1958), where the negative after-potential was explained by the accumulation of potassium near the membrane. On the other hand, the negative after-potentials would not add, on repetitive stimulation, if they were not caused by such an accumulation of any substance. Examples may be provided by DDT-poisoned cockroach giant axons, in which the negative after-potential is greatly augmented (Narahashi & Yamasaki, 1960*b*), and by skeletal muscle fibres of the frog (Ishiko & Sato, 1956)

The records of Fig. 8 were taken in 150 mM-Na + 43 mM-Ba. A large negative after-potential appeared after a single response (record *A*). Upon repetitive stimulation at a frequency of 200/sec, there was little, if any, addition of the negative after-potentials (record *B*). By increasing the stimulus frequency up to 500 /sec, there appeared a slight addition (record *C*). Such a small addition is rather comparable to that observed in the normal axon (Fig. 2 in Narahashi & Yamasaki, 1960*a*), and, therefore, can be accounted for by the accumulation of released potassium in the immediate vicinity of the nerve membrane.

The absence of marked addition of the negative after-potentials on

repetitive stimulation is more clearly seen in Fig. 9, in which the decay of the negative after-potentials of the first through fourth and sixteenth impulses are plotted on a semi-logarithmic scale against time as was done in the previous papers (Narahashi & Yamasaki, 1960*a*, *b*). The open circles show the calculated values for the negative after-potentials which would be expected if they added in a linear manner. The actual small addition of the negative after-potentials seen in this figure falls far short of the calculated addition.

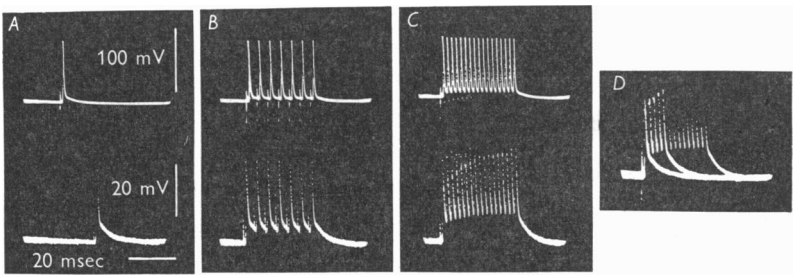

Fig. 8. Records of the action potentials produced by single and repetitive shocks in 150 mM-Na+43 mM-Ba. The frequencies of repetitive stimulation are 200/sec in *B* and 500/sec in both *C* and *D*. Record *D* is a superimposed photograph with varying numbers of stimuli. The lower voltage calibration also applies to *D*. Axon 22. Temperature 28° C.

Time constant of membrane. The measurement of the time constant of decay of the negative after-potential should throw some light on the mechanism of its production, because it is of importance to know whether or not the decay is passive in nature. Record *D* in Fig. 8 is a superimposed photograph with varying numbers of stimuli. It seems at first sight that the decay is almost the same regardless of the number of impulses. Figure 9 reveals this point clearly. Unlike the normal axon, in which the negative after-potential could be expressed as a single exponential term (Narahashi & Yamasaki, 1960*a*), the initial exponential phase was terminated in a faster phase. The time constants of the initial phase in this particular fibre were 5·3 msec (1st impulse), 5·0 msec (2nd), 4·9 msec (3rd and 4th) and 4·6 msec (16th), and those of the terminal phase 3·1 msec (1st impulse), 3·0 msec (2nd) and 2·2 msec (3rd, 4th and 16th), there being a slight but definite tendency for both time constants to decrease with increasing number of stimuli. The same tendency was always seen in other Ba-treated fibres, and is in sharp contrast with the normal axon where the reverse tendency is observed (Narahashi & Yamasaki, 1960*a*). This problem will be discussed later.

The time constant of the initial falling phase of the negative after-potential in a single impulse is given in Table 4. The mean value is calculated as 4·7 msec.

In order to determine the resting membrane time constant of the Ba-treated axon, measurements were made on the rising phase of the

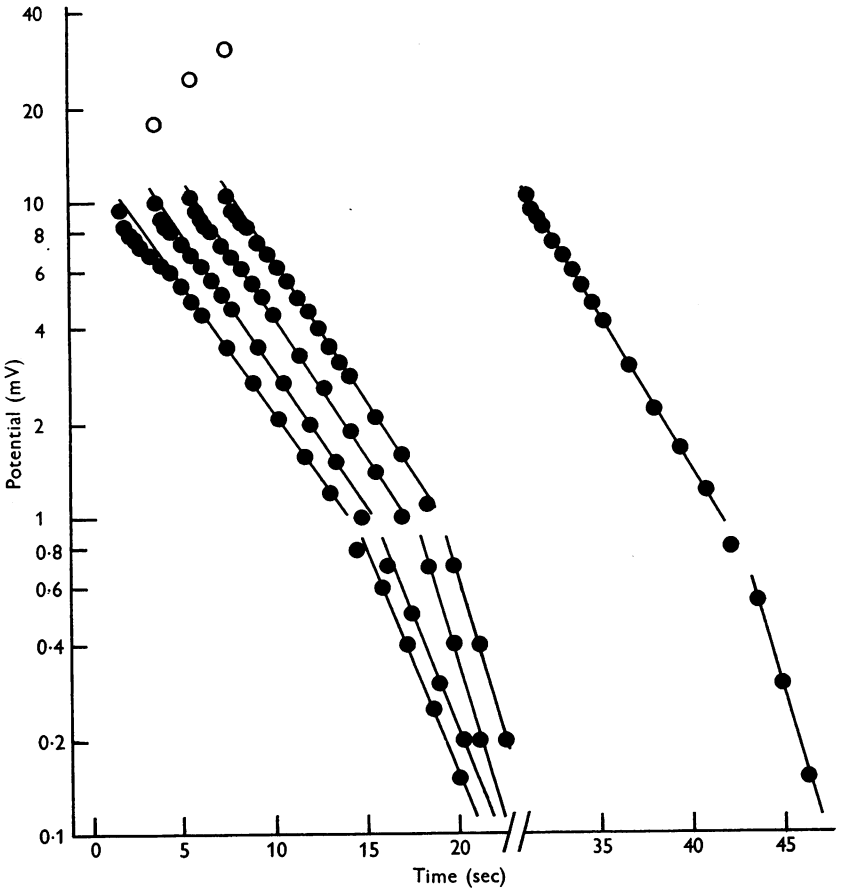

Fig. 9. Time course of the decay of the negative after-potential during a train of impulses at 500/sec in 150 mM-Na+43 mM-Ba. The first, second, third, fourth and sixteenth impulses are illustrated. The ordinate represents the potential on a logarithmic scale, and the abscissa is the time measured from the beginning of the train. The filled circles are the measured points. The straight lines were drawn by eye. The time constants of the initial phase and of the terminal phase (in parentheses) are: 1st, 5·3 msec (3·1 msec); 2nd, 5·0 msec (3·0 msec); 3rd and 4th, 4·9 msec (2·2 msec); 16th, 4·6 msec (2·2 msec). The open circles represent the potential immediately after the end of the second, third and fourth spikes, calculated by adding the initial height of the first negative after-potential to the potential remaining at the moment when the next spike arises. Axon 22. Temperature 28° C.

anelectrotonic potential produced by a weak inward current. Anelectrotonic potentials having a steady-state magnitude of about 10 mV were chosen for measurements, because the membrane resistance became somewhat greater with increasing anodal current, thereby making the time constant larger than its resting value. The time to reach 84 % of the steady-state magnitude was taken as a measure of the time constant, because the time course of the electrotonic potential was regarded as an error function (Hodgkin & Rushton, 1946) under the present experimental conditions. The time constants are shown in Table 4, the mean value being 14·0 msec. This value is nearly three times as large as the time constant of the negative after-potential, which suggests that the falling phase of the negative after-potential is affected by some accelerating mechanism.

TABLE 4. Time constants (msec)

Axon no.	Temp. (°C)	Decay of negative after-potential	Decay of catelectrotonic potential of various amplitudes				Rise of anelectrotonic potential
			2 mV	5 mV	10 mV	20 mV	
18	29·5	3·7	6·5	5·9	4·8	2·6	14·4
19	29·5	4·4	4·3	4·0	3·4	2·3	15·5
22	28	4·5	6·0	5·6	5·1	4·1	10·7
		4·1	7·0	7·0	7·0	7·0	—
		5·3	8·1	7·8	7·3	6·4	15·7
26	32·5	6·0	5·9	5·7	5·4	4·4	16·2
28	30	5·2	3·4	3·4	3·4	3·4	11·6
		—	3·5	3·4	3·3	3·1	—
Mean	29·9	4·7	5·6	5·4	5·0	4·2	14·0

The time constant of decay of the negative after-potential in a single impulse was obtained from the slope of the initial phase of decay drawn on a semi-logarithmic scale as shown in Fig. 9. The time to fall to 16 % of the steady-state amplitude was taken as a measure of the constant of decay of the catelectrotonic potential. The measurements of the catelectrotonic potentials with various magnitudes were plotted against depolarization as in Fig. 11, and the values at each depolarization listed were obtained from the straight line of the graph. The time to reach 84 % of the steady-state amplitude was taken as a measure of the time constant of rise of the anelectrotonic potential. About 10 mV hyperpolarization was employed.

As the next step, the time constant was measured on the falling phase of a catelectrotonic potential. A series of records of catelectrotonic potentials with varying magnitudes was taken as shown in Fig. 10. The time constants measured from such records are plotted against depolarization in Fig. 11. It is seen that they become smaller with depolarization in a linear manner. From such a straight line, the time constants were picked out at depolarizations of 2, 5, 10 and 20 mV, and are listed in Table 4. There is agreement in the order of size of the time constant between the negative after-potential and the catelectrotonic potential, both of which had much smaller time constants than that of the anelectrotonic potential. This seems to imply

that the acceleration of the falling phase of the negative after-potential is related to a depolarization of the membrane.

Voltage–current relation. From the data so far described it seems probable that the mechanism by which the falling phase of the action potential is accelerated is somewhat inhibited by barium, thereby causing the

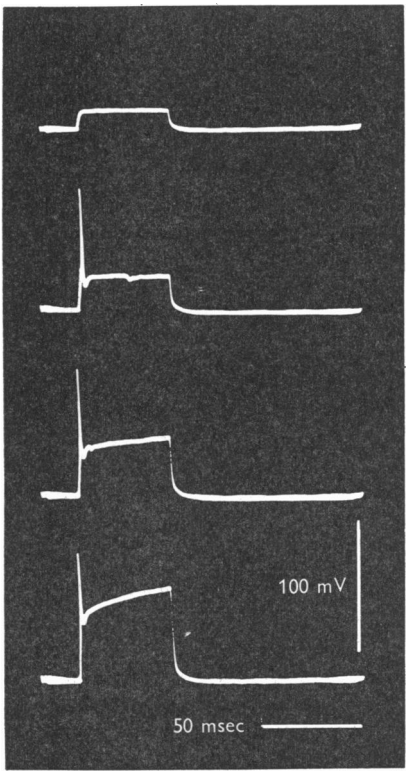

Fig. 10. Records of catelectrotonic potentials of various magnitudes in 150 mM-Na + 43 mM-Ba. Axon 28. Temperature 30° C.

negative after-potential to increase. The mechanism presumably involves the rise in membrane potassium conductance and the inactivation of the sodium-carrying system (Hodgkin & Huxley, 1952*b*). If any effect on the rise in potassium conductance were responsible for the increase in negative after-potential, the voltage–current relation would be changed.

Figure 12 shows a series of records of the catelectrotonic and anelectrotonic potentials in 150 mM-Na (records *A* and *B* respectively) and in 150 mM–Na + 43 mM-Ba (records *C* and *D*). The membrane showed clearly a delayed rectification in 150 mM-Na, which is in accordance with the previous observations (Yamasaki & Narahashi, 1959*b*). It should be

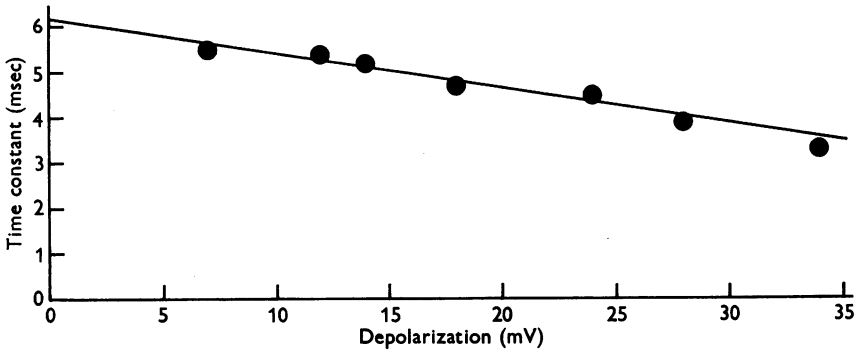

Fig. 11. The relation between the magnitude of depolarization (abscissa) and the time constant of decay of the catelectrotonic potential (ordinate) in 150 mM-Na+43 mM-Ba. The straight line was drawn by eye. Axon 26. Temperature 32·5° C.

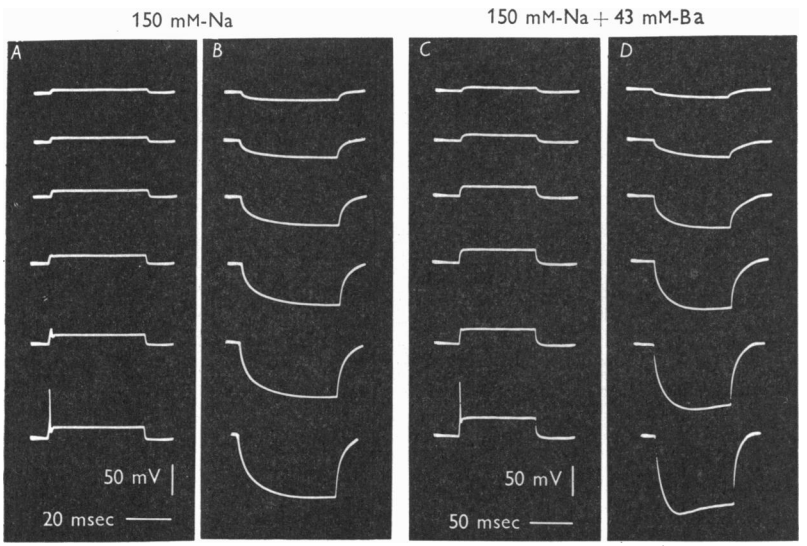

Fig. 12. Records of the catelectrotonic (*A* and *C*) and anelectrotonic (*B* and *D*) potentials in 150 mM-Na and in 150 mM-Na+43 mM-Ba. The current strengths were: *A* (from top to bottom), 1·15, 2·18, 2·87, 3·91, 5·17, and $6{\cdot}90 \times 10^{-8}$ A; *B*, 1·38, 2·07, 3·27, 4·60, 5·75, and $7{\cdot}98 \times 10^{-8}$ A; *C*, 0·58, 0·92, 1·97, 3·24, 4·64 and $6{\cdot}49 \times 10^{-8}$ A; *D*, 0·46, 0·92, 2·14, 3·48, 4·87 and $8{\cdot}44 \times 10^{-8}$ A. Axon 26. Temperature 32·5° C.

added that no repetitive excitation occurred either in 150 mM-Na or in 150 mM-Na + 43 mM-Ba even when the intensity of cathodal current was raised to two or three times threshold.

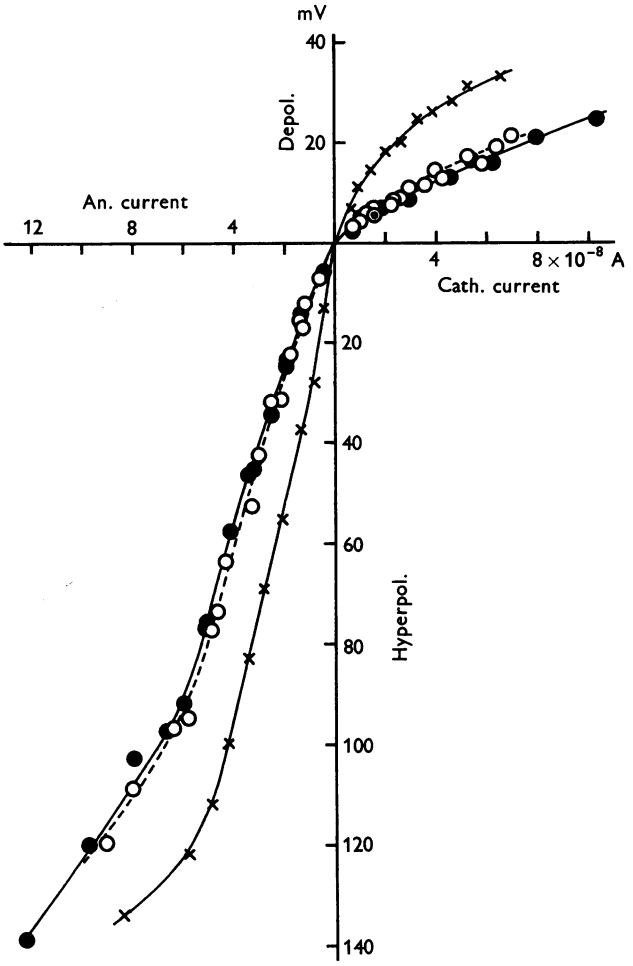

Fig. 13. Voltage–current relations. Measurements were made at first in 150 mM-Na (●), next in 150 mM-Na + 43 mM-Ba (×), and then again in 150 mM-Na (○). The abscissa represents the current strength and the ordinate the potential. Axon 26. Temperature 32·5° C.

The magnitudes of the steady-state electrotonic potentials are plotted against the current strengths in Fig. 13. The filled circles show the control measurements made in 150 mM-Na. It should be noted that the effective resistance across the membrane shown by the slope of the curve is reduced not only by depolarization but also by hyperpolarization greater

than about 100 mV. The crosses represent the measurements in 150 mM-Na + 43 mM-Ba. As is clearly shown by the change in slope, the effective resistance greatly increases both for depolarized and for hyperpolarized membranes, except at the largest hyperpolarization employed, although the delayed rectification is still observed. When the nerve was again washed with the 150 mM-Na solution, the voltage–current relation was completely restored (open circles).

TABLE 5. Effective membrane resistance (kΩ)

		At resting potential			At a depolarization of 10 mV			At a depolarization of 20 mV	
Axon no.	Temp. (°C)	Normal Ringer's solution	150 mM-Na	150 mM-Na + 43 mM-Ba	Normal Ringer's solution	150 mM-Na	150 mM-Na + 43 mM-Ba	150 mM-Na	150 mM-Na + 43 mM-Ba
21	28	620	—	—	220	—	—	—	—
22	28	770	—	2000	410	—	850	—	710
		1330	—	2500	520	—	820	—	600
23	31	—	660	1250	—	190	260	130	110
24	31	—	830	—	—	250	—	160	—
25	32·5	—	800	—	—	160	—	—	—
26	32·5	—	1100	—	—	250	—	210	—
		—	1270	2630	—	280	930	200	480
		—	1280	—	—	290	—	290	—
27*a*	30	—	800	—	—	170	—	110	—
27*b*	30	—	780	—	—	150	—	—	—
28	30	—	820	1950	—	260	970	160	290
		—	—	1610	—	—	490	—	240
Mean	30·3	910	930	1990	380	220	720	180	410

From voltage-current curves such as that shown in Fig. 13, effective resistances across the membrane were calculated and are listed in Table 5. The resting effective resistance refers to the slope at the point where no current is passed. The effective resistance was also measured at depolarizations of 10 and 20 mV. The increase in effective resistance caused by barium amounts to about twice in the resting membrane and about twice to three times in the depolarized membrane.

Since the membrane effective resistance (R_e) is related to membrane resistance (the resistance times unit length of the membrane, r_m) and axoplasm resistance (the resistance per unit length of the axoplasm, r_i) by the equation $R_e = \frac{1}{2}\sqrt{(r_m r_i)}$, the relative change in the membrane resistance caused by depolarization or hyperpolarization can be computed from the voltage–current curve, if the axoplasm resistance is assumed to remain constant. Such calculated curves are shown in Fig. 14, in which it is seen that the Ba-treated axon has a membrane resistance much higher than normal at all depolarizations.

An attempt was made to calculate current density from the voltage–current curve of Fig. 13. By the current density is meant current per unit area of membrane which would result from a uniform change in

potential (V) over the whole length of the fibre. According to Cole & Curtis (1941), the current density (i) is proportional to $I.\mathrm{d}I/\mathrm{d}V$, where I is current intensity passed through the membrane. As has been shown by Burke & Ginsborg (1956), if the specific resistance of the axoplasm (R_i) and the diameter of the fibre (d) are known,

$$i = \frac{R_i}{\pi^2 d^3} I \frac{\mathrm{d}I}{\mathrm{d}V}.$$

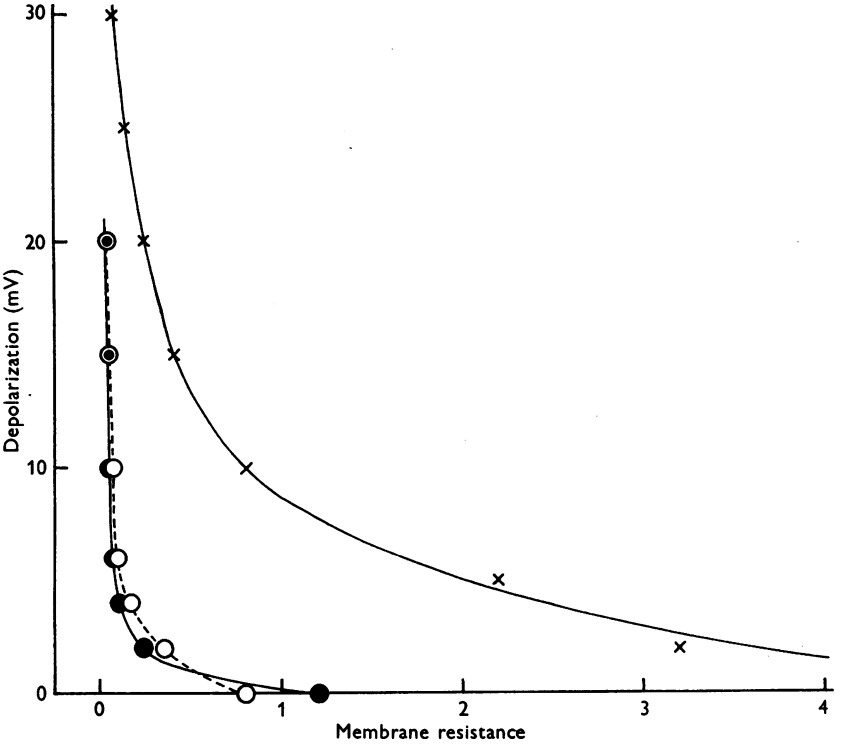

Fig. 14. The relation between membrane resistance in arbitrary units (abscissa) and the magnitude of depolarization (ordinate) calculated from the curves of Fig. 13. Measurements were made first in 150 mM-Na (●), next in 150 mM-Na+43 mM-Ba (×), and then again in 150 mM-Na (○).

The calculated curves are drawn in Fig. 15, in which the abscissa represents the displacement of the membrane potential from the resting level, and the ordinate the current density in arbitrary units. If the specific axoplasm resistance and the fibre diameter are assumed to be 130 Ω cm and 50 μ respectively (Yamasaki & Narahashi, 1959*b*), each unit of current density would be equivalent to about 10 μA/cm^2. The current density is shown to be very much reduced by barium both in depolarized and in hyperpolarized membranes.

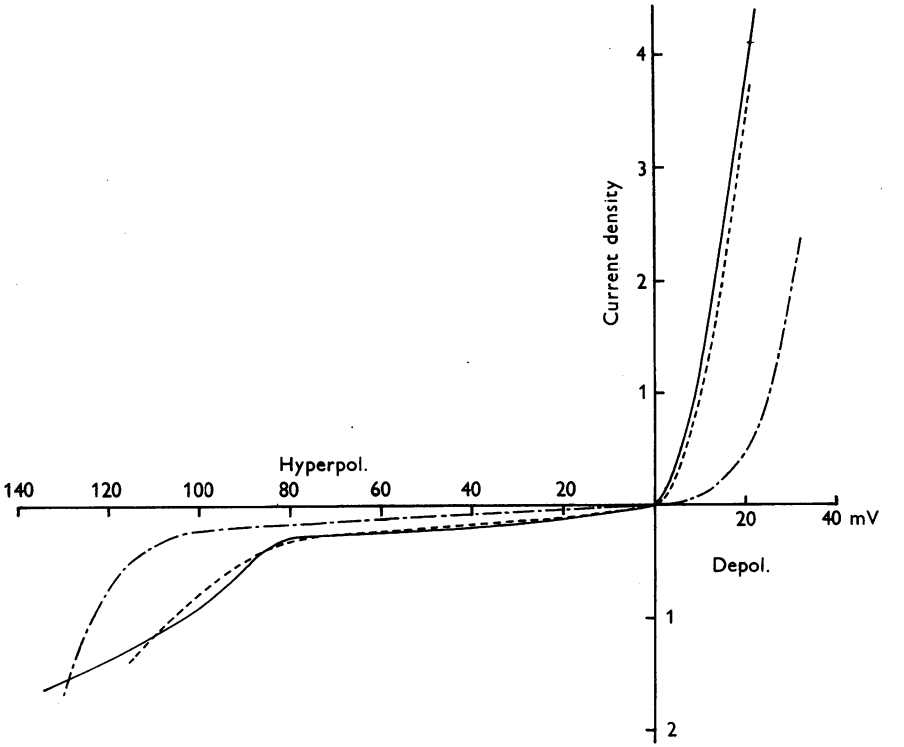

Fig. 15. The relation between the displacement of membrane potential from the resting level (abscissa) and the current density (ordinate) in arbitrary units, i.e. currents per unit area of membrane which would result from a uniform change in potential over the whole length of the axon. The curves were calculated from Fig. 13. Measurements were made first in 150 mM-Na (———), next in 150 mM-Na + 43 mM-Ba (—·—·—), and then again in 150 mM-Na (– – – –).

Transmembrane stimulation in isotonic Ba solutions

It has already been pointed out that the isotonic barium medium causes conduction block. However, it remains to be seen whether under these conditions the membrane is capable of producing responses that fail to conduct along the axon. This problem has not been examined in detail, and only the results of preliminary experiments will be described here.

Records of the electrotonic potential of the axon bathed in isotonic barium are shown in Fig. 16. No spike potential was generated even when the membrane was depolarized by as much as 120 mV (record *A*). Record *B* in Fig. 16, which was taken with a faster sweep, shows the rising phase of the catelectrotonic potential more clearly. There is a step in the early part of the rising phase which at first sight might seem to be a local

response. However, this possibility was excluded by superposing the catelectrotonic potential on the anelectrotonic one (record *C*) produced by the same but opposite currents, because both rising phases just coincided and no extra potential was seen during the course of the catelectrotonic potential. Therefore, it is reasonable to assume that the step indicates the onset of delayed rectification.

The small potentials seen during the course of the largest catelectrotonic potential (Fig. 16 *B*) are likely to be electrotonic spread of the action potentials produced in the intact region of the nerve cord, because the nerve sheath behaves as a strong barrier against the penetration of ions (Yamasaki & Narahashi, 1959*a*).

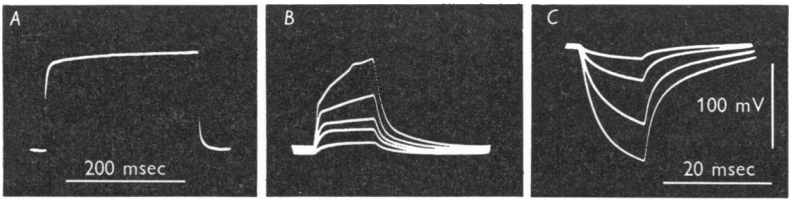

Fig. 16. Records of the catelectrotonic (*A* and *B*) and anelectrotonic (*C*) potentials in isotonic Ba. *B* and *C* are superimposed records, in which the intensity of applied current is changed at random. Axon 28. Temperature 30° C.

DISCUSSION

Unlike crustacean muscle fibres (Fatt & Ginsborg, 1958) and mammalian B and C fibres (Greengard & Straub, 1959), the giant axons of the cockroach are unable to produce action potentials in an isotonic barium solution resembling in this respect mammalian A fibres (Greengard & Straub, 1959). However, the action of barium, to increase and prolong the falling phase of the action potential seen with crustacean muscles and mammalian B and C fibres, has also been demonstrated in cockroach giant axons with rather weak concentrations of barium. The increase in the negative afterpotential caused by weak concentrations of barium was also observed in frog nerve (Lorente de Nó & Feng, 1946).

The increase in resting membrane resistance caused by barium is consistent with the fall of resting potential. Assuming that the resting membrane conductance is largely but not exclusively due to potassium conductance (Yamasaki & Narahashi, 1959*a*), the decrease in the latter should cause depolarization.

It seems likely that the slowness of the rise of the action potential caused by barium is due to a depression of the sodium-carrying system. The rise in the critical level of depolarization is consistent with this view.

The fact that the active membrane potential and the rate of rise of the action potential are stabilized by barium against the displacement of the membrane potential shows that the inactivation of the sodium-carrying system normally occurring upon depolarization does not take place. In other words, under the influence of barium, the sodium-carrying system is largely stabilized at a half depressed state, so that its rapid availability for carrying sodium ions upon depolarization is reduced, thereby slowing down the rate of rise of the action potential, and so that after activation its inactivation proceeds very slowly, contributing towards slowing down the rate of fall of the action potential. The fact that the spike height is not reduced by barium does not seem to be inconsistent with this view, because the delay of the inactivation occurring upon depolarization together with the decrease in potassium conductance rise, which will be discussed later, would enable the membrane to be depolarized as far as or even beyond the normal level.

The increase in negative after-potential caused by barium cannot be explained in terms of the accumulation of any substance near the membrane, because no linear addition of the negative after-potentials occurs during repetitive excitation. In barium the membrane resistance is considerably higher than normal not only in the resting state but also in the depolarized membrane. This leads us to the assumption that the potassium conductance, which rises with a certain delay upon depolarization, is still less than normal at any particular level of depolarization. It follows that the potassium conductance during the falling phase of the action potential is smaller than normal, thereby preventing the falling phase from reaching the resting level at once, forming a large negative after-potential. The depression of the inactivation process normally occurring upon depolarization, which has been discussed in the preceding paragraph, is also likely to be partly responsible for the large negative after-potential. The positive phase following the spike, which is thought to be indicative of the increase in potassium conductance (Yamasaki & Narahashi, 1959*a*), disappears in barium, this effect being also well explained in terms of a smaller potassium conductance.

The falling phase of the catelectrotonic potential has a time constant appreciably smaller than that of the resting membrane. Furthermore, the rate of the falling phase depends partly on the magnitude of depolarization, becoming slightly higher with increasing depolarization. It follows that some accelerating mechanism for the falling phase comes into action when the membrane is depolarized. It is reasonable to suppose that this accelerating mechanism is a rise in potassium conductance. On the other hand, the time constant of the falling phase of the negative after-potential is approximately the same as that of the catelectrotonic potential and

appreciably smaller than that of the resting membrane. This is explained on the assumption that the accelerating mechanism, i.e. the rise in potassium conductance, is still working slightly during the falling phase of the negative after-potential, although the mechanism is now partly suppressed by barium, as mentioned above.

It is worth while to note in this connexion that in barium the falling phase of the negative after-potential is slightly but definitely accelerated upon repetitive stimulation, whereas the reverse is true in normal Ringer's solution (Narahashi & Yamasaki, 1960*a*). This acceleration may be explained as follows. For the first impulse the potassium conductance during the falling phase is still less than normal. By repetitive excitation however, a small additional increase in potassium conductance may occur. Such an increase would accelerate the falling phase of the negative after-potential, thereby making the time constant smaller.

SUMMARY

1. The effect of Ba on the spike potential and the negative after-potential of the cockroach giant axon has been examined by means of intracellular micro-electrodes.

2. Nerve conduction was reversibly blocked by isotonic Ba solution and a solution with 75 mM-Na and 93 mM-Ba.

3. By 21–76 mM-Ba the resting potential was slightly reduced, the rising and falling phases of the action potential were considerably slowed down, and the negative after-potential was markedly increased, the degree of the effects being dependent on the Ba concentration. The spike amplitude slightly increased in weak concentrations of Ba.

4. The critical depolarization for firing became greater but the threshold current remained almost unaltered in 43 mM-Ba.

5. The height and the rate of rise of the action potential were stabilized by 43 mM-Ba, undergoing smaller changes on displacement of the membrane potentials.

6. The negative after-potentials increased by 43 mM-Ba did not add linearly during repetitive excitation.

7. The falling phase of the negative after-potential in 43 mM-Ba could be expressed by two exponential terms. The initial phase, occupying the major part of a negative after-potential, was slower than the terminal phase. Both phases were slightly accelerated by repetitive stimulation.

8. In 43 mM-Ba, the time constants for the falling phase of the negative after-potential and of the catelectrotonic potential were appreciably smaller than the time constant of the resting membrane.

9. The effective membrane resistance was remarkably increased by 43 mM-Ba not only in the resting state but also in the depolarized membrane.

10. In isotonic Ba, neither spikes nor local responses were produced by transmembrane stimulation.

11. The Na-carrying system is to some extent stabilized by Ba at a half depressed state. The increase in negative after-potential caused by Ba can be explained on the assumption that the rise in K conductance during the falling phase of the action potential falls short of the normal level and that the inactivation normally occurring upon depolarization is much depressed, thereby preventing the falling phase from reaching the resting potential at once.

I am indebted to Dr T. Yamasaki for his interest and encouragement during the course of this work. Thanks are also due to Dr S. Hagiwara and Dr A. Watanabe for criticisms, and to Miss S. Hamada for technical assistance. This work was supported in part by a grant from the Ministry of Education of Japan.

REFERENCES

BURKE, W. & GINSBORG, B. L. (1956). The electrical properties of the slow muscle fibre membrane. *J. Physiol.* **132**, 586–598.

COLE, K. S. & CURTIS, H. J. (1941). Membrane potential of the squid giant axon during current flow. *J. gen. Physiol.* **24**, 551–563.

FATT, P. & GINSBORG, B. L. (1958). The ionic requirements for the production of action potentials in crustacean muscle fibres. *J. Physiol.* **142**, 516–543.

FRANKENHAEUSER, B. & HODGKIN, A. L. (1956). The after-effects of impulses in the giant nerve fibres of *Loligo*. *J. Physiol.* **131**, 341–376.

GREENGARD, P. & STRAUB, R. W. (1958). After-potentials in mammalian non-myelinated nerve fibres. *J. Physiol.* **144**, 442–462.

GREENGARD, P. & STRAUB, R. W. (1959). Restoration by barium of action potentials in sodium-deprived mammalian B and C fibres. *J. Physiol.* **145**, 562–569.

HODGKIN, A. L. & HUXLEY, A. F. (1952*a*). The dual effect of membrane potential on sodium conductance in the giant axon of *Loligo*. *J. Physiol.* **116**, 497–506.

HODGKIN, A. L. & HUXLEY, A. F. (1952*b*). A quantitative description of membrane current and its application to conduction and excitation in nerve. *J. Physiol.* **117**, 500–544.

HODGKIN, A. L. & RUSHTON, W. A. H. (1946). The electrical constants of a crustacean nerve fibre. *Proc. Roy. Soc.* B, **133**, 444–479.

ISHIKO, N. & SATO, M. (1956). The negative after-potential of skeletal muscle fibres. *Kumamoto med. J.* **9**, 190–198.

LORENTE DE NÓ, R. & FENG, T. P. (1946). Analysis of the effect of barium upon nerve with particular reference to rhythmic activity. *J. cell. comp. Physiol.* **28**, 397–464.

NARAHASHI, T. (1960*a*). Excitation and electrical properties of giant axon of cockroaches. In *Electrical Activity of Single Cells*, ed. KATSUKI, Y. Tokyo: Igakushoin.

NARAHASHI, T. (1960*b*). Nature of negative after potential of cockroach giant axons and its modification by drugs. *J. Physiol. Soc. Japan*, **22**, 766.

NARAHASHI, T. & YAMASAKI, T. (1960*a*). Mechanism of the after-potential production in the giant axons of the cockroach. *J. Physiol.* **151**, 75–88.

NARAHASHI, T. & YAMASAKI, T. (1960*b*). Mechanism of increase in negative after-potential by dicophanum (DDT) in the giant axons of the cockroach. *J. Physiol.* **152**, 122–140.

NARAHASHI, T. & YAMASAKI, T. (1960*c*). Behaviors of membrane potential in the cockroach giant axons poisoned by DDT. *J. cell. comp. Physiol.* **55**, 131–142.

SHANES, A. M. (1958). Electrochemical aspects of physiological and pharmacological action in excitable cells. Part II. The action potential and excitation. *Pharmacol. Rev.* **10**, 165–273.

WEIDMANN, S. (1955). The effect of the cardiac membrane potential on the rapid availability of the sodium-carrying system. *J. Physiol.* **127**, 213–224.

YAMASAKI, T. & NARAHASHI, T. (1958). Effects of potassium and sodium ions on the resting and action potentials of the giant axon of the cockroach. *Nature, Lond.*, **182**, 1805.

YAMASAKI, T. & NARAHASHI, T. (1959*a*). The effects of potassium and sodium ions on the resting and action potentials of the cockroach giant axon. *J. insect Physiol.* **3**, 146–158.

YAMASAKI, T. & NARAHASHI, T. (1959*b*). Electrical properties of the cockroach giant axon. *J. insect Physiol.* **3**, 230–242.